BIOCHEMISTRY
including biophysical chemistry & molecular biology

Article

pubs.acs.org/biochemistry

Carboxyl Group of Glu113 Is Required for Stabilization of the Diferrous and Bis-Fe^{IV} States of MauG

Nafez Abu Tarboush,[†] Erik T. Yukl,[‡] Sooim Shin,[§] Manliang Feng,[∥] Carrie M. Wilmot,[‡] and Victor L. Davidson*[,§]

[†]Biochemistry and Physiology Department, College of Medicine, The University of Jordan, Amman, Jordan 11942

[‡]Department of Biochemistry, Molecular Biology and Biophysics, University of Minnesota, Minneapolis, Minnesota 55455, United States

[§]Burnett School of Biomedical Sciences, College of Medicine, University of Central Florida, Orlando, Florida 32827, United States

[∥]Department of Chemistry, Tougaloo College, Tougaloo, Mississippi 39174, United States

Supporting Information

ABSTRACT: The diheme enzyme MauG catalyzes a six-electron oxidation required for post-translational modification of a precursor of methylamine dehydrogenase (preMADH) to complete the biosynthesis of its protein-derived tryptophan tryptophylquinone (TTQ) cofactor. Crystallographic studies have implicated Glu113 in the formation of the bis-Fe^{IV} state of MauG, in which one heme is Fe^{IV}═O and the other is Fe^{IV} with His-Tyr axial ligation. An E113Q mutation had no effect on the structure of MauG but significantly altered its redox properties. E113Q MauG could not be converted to the diferrous state by reduction with dithionite but was only reduced to a mixed valence Fe^{II}/Fe^{III} state, which is never observed in wild-type (WT) MauG. Addition of H_2O_2 to E113Q MauG generated a high valence state that formed more slowly and was less stable than the bis-Fe^{IV} state of WT MauG. E113Q MauG exhibited no detectable TTQ biosynthesis activity in a steady-state assay with preMADH as the substrate. It did catalyze the steady-state oxidation of quinol MADH to the quinone, but 1000-fold less efficiently than WT MauG. Addition of H_2O_2 to a crystal of the E113Q MauG-preMADH complex resulted in partial synthesis of TTQ. Extended exposure of these crystals to H_2O_2 resulted in hydroxylation of Pro107 in the distal pocket of the high-spin heme. It is concluded that the loss of the carboxylic group of Glu113 disrupts the redox cooperativity between hemes that allows rapid formation of the diferrous state and alters the distribution of high-valence species that participate in charge-resonance stabilization of the bis-Fe^{IV} redox state.

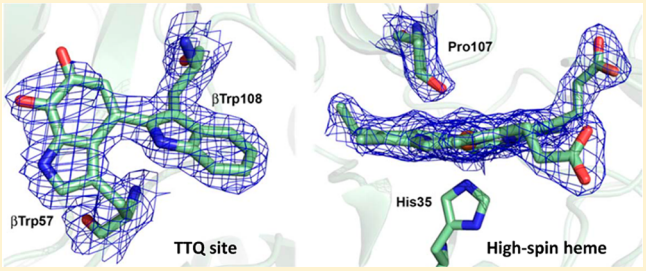

A 42-kDa *c*-type diheme enzyme,[1] MauG catalyzes the final steps in the biosynthesis of the protein-derived cofactor[2,3] tryptophan tryptophylquinone (TTQ) in methylamine dehydrogenase (MADH).[4] In order to complete TTQ formation, these post-translational modifications require a six-electron oxidation of a precursor of methylamine dehydrogenase (preMADH) that possesses a monohydroxylated residue *β*Trp57[5,6] (Figure 1). The order of the reactions that MauG catalyzes are covalent cross-linking of *β*Trp57 to *β*Trp108, insertion of a second oxygen atom into the side chain of *β*Trp57, and oxidation of the quinol species to the quinone.[7] Diferric MauG can be oxidized by H_2O_2 to generate the high-valence heme species required for TTQ biosynthesis. In contrast to peroxidases and other heme-dependent oxygenases, the high-valent species generated in MauG is not compound I or compound ES, but a bis-Fe^{IV} intermediate of MauG[8] in which one heme is present as Fe^{IV}═O with an axial ligand provided by a His and the other is present as Fe^{IV} with His-Tyr axial ligation and no exogenous bound ligand.[9] Experimental and computational studies have demonstrated that Tyr294,

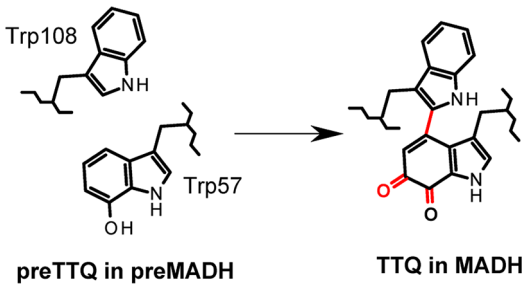

Figure 1. MauG-catalyzed TTQ biosynthesis from preMADH. The post-translational modifications of preMADH that are catalyzed by MauG are highlighted in red.

which provides an axial ligand for the six-coordinate heme iron, plays a critical role in stabilization of the bis-Fe^{IV} state.[10−13]

Received: July 9, 2013
Revised: August 15, 2013
Published: August 18, 2013

dx.doi.org/10.1021/bi400905s | *Biochemistry* 2013, 52, 6358−6367

The bis-Fe^{IV} species is also stabilized by an unusual charge-resonance transition in which the two Fe^{IV} hemes and Trp93, which resides between the two hemes, share spin and charge via ultrafast hopping-mediated electron transfer.[14] The crystal structure of a catalytically competent complex of MauG and preMADH from *Paracoccus denitrificans* has been determined,[9] and it shows that the process of MauG-dependent TTQ biosynthesis requires long-range electron transfer, as the distances between the residues of preMADH that are modified to form TTQ and each heme iron of MauG are approximately 40.1 and 19.4 Å. Trp199 of MauG resides at the site of interaction with preMADH and is positioned approximately halfway between βTrp108 and the nearest heme of MauG. Site-directed mutagenesis and kinetic and thermodynamic analyses showed that Trp199 mediates a hole-hopping mechanism of electron transfer that is required for MauG-dependent TTQ biosynthesis.[15,16] As the details of this mechanism of remote catalysis by MauG are being elucidated, questions remain concerning the roles of specific amino acid residues that are in close proximity to the hemes in stabilizing the different redox states of MauG.

Inspection of the crystal structure of MauG identified three residues of interest in the distal pocket of the high-spin five-coordinate heme: Pro107, Gln103, and Glu113. The results of site-directed mutagenesis studies of Pro107[17] showed that the presence of Pro107 is critical in maintaining the proper structure of the distal pocket of the high-spin heme of MauG, controlling the binding of exogenous ligands and directing the reactivity of the heme-activated oxygen during catalysis, thus minimizing the oxidation of other residues of MauG. A quantum chemical investigation that explored the unusual Mössbauer spectroscopic parameters of the bis-Fe^{IV} MauG suggested that Gln103 is important in stabilizing the Fe^{IV}=O by hydrogen bonding to the oxo.[13] On the basis of the crystal structure of NO bound to the MauG-preMADH complex,[18] it was suggested that Glu113 may be important in promoting cleavage of the O−O bond through protonation of oxygen intermediates bound to heme during catalysis. An analogous role has been suggested for a Glu in the same spatial position in the heme pocket of certain peroxidases.[19−22]

In this study, Glu113 was converted to glutamine. While this results in no significant structural changes to MauG, the E113Q mutation dramatically affects the redox properties of MauG and its TTQ biosynthesis activity. It is concluded that the loss of the carboxylic group of Glu113 disrupts the redox cooperativity between the hemes of MauG that allows rapid formation of the diferrous redox state[23] and alters the distribution of high valence species that participate in charge-resonance stabilization of the bis-Fe^{IV} redox state. The interpretation of these results has implications for understanding not only the structure−function relationships of MauG but also for peroxidases and heme-dependent oxidative enzymes in general.

EXPERIMENTAL PROCEDURES

Protein Expression and Purification. Recombinant MauG[1] and preMADH[5] were purified from *P. denitrificans* and *Rhodobacter sphaeroides*, respectively, as described previously. Glu113 of MauG was converted to Gln by site-directed mutagenesis of double-stranded pMEG391, which contains *mau*G, using the QuikChange kit (Strategene). E113Q MauG was expressed in *P. denitrificans* and isolated from the periplasmic fraction as described for recombinant wild-type (WT) MauG.[1]

Redox Titrations. E_m values of E113Q MauG were determined by anaerobic spectrochemical titration, as described previously for WT MauG using FMN as a mediator.[23] Sodium dithionite and potassium ferricyanide were used in reductive and oxidative titrations, respectively. The fraction of MauG that was reduced was determined by comparison with the spectra of the completely oxidized and reduced forms of MauG and quantitated from the absorbance at 550 nm. Data were fit to the Nernst equation (eq 1) and eq 2, which describes the redox behavior of a system with two redox active centers, where a is the fraction of the total absorbance change attributable to one center and $(1 - a)$ is the fraction of the total absorbance change attributable to the other.

$$E = E_m + (2.3RT/nF)\log([\mathrm{MauG_{oxi}}]/[\mathrm{MauG_{red}}]) \quad (1)$$

$$\text{fraction reduced} = a/[1 + 10^{((E-E_{m1})/0.059\mathrm{V})}] + (1 - a)/[1 + 10^{((E-E_{m2})/0.059\mathrm{V})}] \quad (2)$$

Resonance Raman Spectroscopy. Resonance Raman spectra were recorded using a Raman spectrometer consisting of a Spex model 1877 triple spectrograph and a CCD detector as reported previously.[23] A 406.7 nm line from an argon−krypton ion laser (Spectra-Physics BeamLok model 2080-KV) was used as the excitation source, and the Raman signal was collected in a 120° geometry. The laser power was adjusted to ~5 mW at the sample. Each spectrum was recorded with a 60 s accumulation time, and 10 repetitively measured spectra were averaged to improve the quality of the final spectrum. The frequencies of the Raman bands were calibrated using the standard spectrum of cyclohexane. Samples contained 0.15 mM protein in 0.05 M potassium phosphate buffer, pH 7.5, and spectra were recorded at 25 °C.

Steady-State Kinetic Assay. Steady-state kinetic studies of MauG-dependent TTQ biosynthesis from preMADH[17,24] and from quinol MADH[24] were performed using previously described spectrophotometric assays. E113Q MauG was mixed with preMADH in 0.01 M potassium phosphate buffer, pH 7.5 at 25 °C. Reactions were initiated by addition of 100 μM H_2O_2, and the rate of appearance of quinone MADH was monitored at 440 nm. The data were fit by eq 3.

$$v/E = k_{cat}[S]/([S] + K_m) \quad (3)$$

Mass Spectrometry. Samples were desalted and exchanged into 75:25 acetonitrile/water, 0.1% formic acid using C4 resin ZipTip pipet tips (Millipore) prior to introduction into the mass spectrometer. Data were acquired on a QSTAR XL (AB Sciex) quadrupole time-of-flight mass spectrometer with the IonSpray electrospray source. Samples were manually injected into a 10-μL sample loop plumbed into the divert/inject valve of the instrument. Samples were infused at a flow rate of 10 μL/min with 50:50 acetonitrile/water, 0.1% formic acid. The IonSpray voltage was 4700 V. The TOF region acceleration voltage was 4 kV, and the injection pulse repetition rate was 4.9 kHz. The monoisotopic peaks of human renin substrate tetradecapeptide from Sigma-Alrdich (St. Louis, MO) were used for external calibration ($[M + 3H]^{3+}$ at 586.9830 and $[M + 2H]^{2+}$ at 879.9705). TOF MS spectra were acquired from 700 to 2200 m/z for approximately 5 min with a 1 s accumulation time. The acquisition software was Analyst QS v1.0 (AB Sciex). The Bayesian protein reconstruct tool in BioAnalyst extensions v1.1

dx.doi.org/10.1021/bi400905s | *Biochemistry* 2013, 52, 6358−6367

(AB Sciex) was used for multiple charge state data deconvolution of the intact proteins.

Crystallization and X-ray Structure Determination of the E113Q MauG-preMADH Complex. A 2:1 E113Q MauG/preMADH ratio mix (100/50 μM) corresponding to the stoichiometry observed in the molecular complex of WT MauG/preMADH was used. The protein complex crystallized through optimization of the conditions previously established for WT MauG/preMADH[9] by hanging drop vapor diffusion in VDX plates (Hampton Research). Single crystals suitable for X-ray data collection were obtained from drops assembled with 1 μL of protein solution layered with 3 μL of reservoir solution over a 22−26% w/v PEG 8000, 0.1 M sodium acetate, 0.1 M MES pH 6.4 reservoir. Crystals were cryoprotected as described previously through the inclusion of 10% PEG 400.[9] The H_2O_2-treated crystals were prepared by soaking in cryoprotectant solution containing 2 mM H_2O_2 for 2 min prior to cryo-cooling. X-ray diffraction data were collected at GM/CA-CAT beamlines 23-ID-D and 23-ID-B of the Advanced Photon Source, Argonne National Laboratory, Argonne, IL. Data were collected at 100 K using a beam size matching the dimensions of the largest crystal face.

The diffraction data are essentially isomorphous with data obtained from WT MauG/preMADH crystals in the space group *P*1 with one complex (two E113Q MauGs bound to one preMADH) in the asymmetric unit. The data were processed with HKL2000,[25] and structure solutions were obtained by difference Fourier using the coordinates of WT MauG/preMADH (PDB entry 3L4M) retaining only the protein components and with Glu113 mutated to Gln. Refinement was carried out using REFMAC[26] in the CCP4 program suite,[27] and model-building was carried out in COOT.[28] Restrained refinement with TLS was carried out using no distance restraints between the heme iron centers and their ligands. Refinement was assessed as complete when the $F_o - F_c$ electron density contained only noise.

RESULTS

Effects of the E113Q Mutation on the Spectroscopic Properties of the Oxidized and Reduced Forms of MauG. The absorbance spectrum of diferric E113Q MauG is similar to that of WT MauG except for a 2 nm red shift of the Soret peak maximum and a slight broadening of the Soret peak (Figure 2). Anaerobic reductive titration of WT MauG with dithionite requires two electron equivalents and yields the spectrum of the diferrous enzyme with an increase in intensity and red shift of the Soret peak to 418 nm with a shoulder at 427 nm and appearance of the α and β bands at 550 and 524 nm, respectively.[1] Titration of E113Q MauG yielded different results. The reductive titration of E113Q MauG with dithionite was complete after addition of only one electron equivalent, and further addition of dithionite resulted in no additional spectral changes. In the resulting spectrum (Figure 2B) the Soret peak shifts slightly to 412 nm without an increase in intensity and with a more pronounced shoulder at 427 nm, and the α and β bands are poorly resolved.

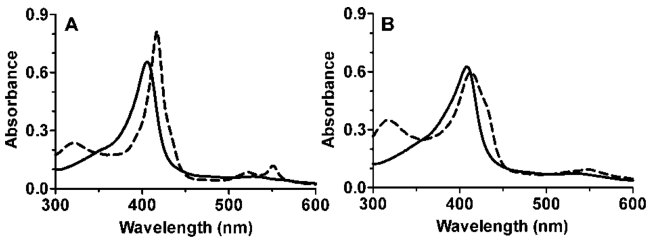

Figure 2. Absorption spectra of oxidized and reduced WT MauG and E113Q MauG. (A) Overlay of the spectra of 2 μM diferric WT MauG before (solid line) and after (dashed line) reduction by sodium dithionite. (B) Overlay of the spectra of 2 μM diferric E113Q MauG before (solid line) and after (dashed line) reduction by sodium dithionite.

It was previously shown that in diferric WT MauG one heme is low-spin and the other is high-spin.[1] While it is difficult to distinguish the spin states of the hemes by absorbance spectroscopy, the spin states of each heme in the diferric and diferrous redox states may be determined by resonance Raman spectroscopy (Figure 3). An advantage of this approach is that the spectra may be recorded in the solution state to correlate with the absorbance spectra and activity studies. Bands in the resonance Raman spectrum are known to be sensitive to oxidation state and spin state.[29−31] The spectra of diferric WT MauG and E113Q MauG are essentially identical. In each, the oxidation state marker band (ν_4) is centered at 1374 cm^{-1}, indicating that both hemes are in the ferric state. Each spectrum contains ν_3 bands at 1478 and 1501 cm^{-1}, which correspond to the high-spin and low-spin hemes, respectively. After addition of dithionite, the spectra of WT MauG and E113Q MauG were different. The spectrum of WT MauG shows a single ν_4 band that is centered at 1359 cm^{-1}, indicating that both hemes are in the ferrous state and the ν_3 bands have shifted to 1467 and 1492 cm^{-1} for the high-spin and low-spin hemes, respectively. In contrast, the spectrum of E113Q MauG shows two ν_4 bands of equivalent intensity centered at 1359 cm^{-1} and 1374 cm^{-1}. The ν_3 band for the high-spin heme exhibits the same shift as seen in the WT MauG spectrum, indicating that it is ferrous. However, the position of the ν_3 band for the low-spin heme indicates that it is still ferric. These results indicate that the absorption spectrum of dithionite-reduced E113Q MauG (Figure 2B) is of a mixed-valence state with the high-spin heme as Fe^{II} and the low-spin heme as Fe^{III}. While a stable mixed-valence state is a common feature of bacterial diheme

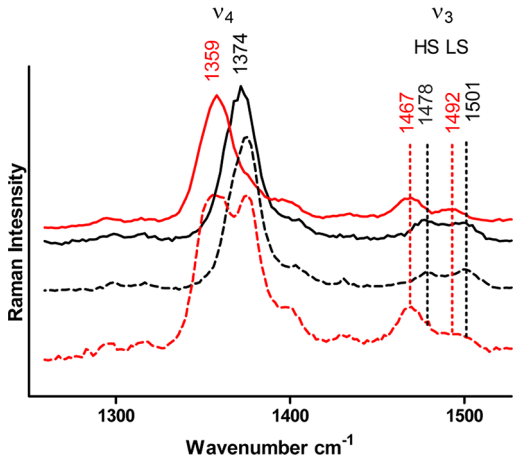

Figure 3. Resonance Raman spectra of oxidized and reduced WT MauG and E113Q MauG. The spectra of the following species are overlaid: diferric E113Q MauG before (black, dashed line) and after reduction by dithionite (red, dashed line) and diferric WT MauG before (black, solid line) and after reduction by dithionite (red, solid line). Marker bands and their frequencies are indicated.

dx.doi.org/10.1021/bi400905s | *Biochemistry* 2013, 52, 6358−6367

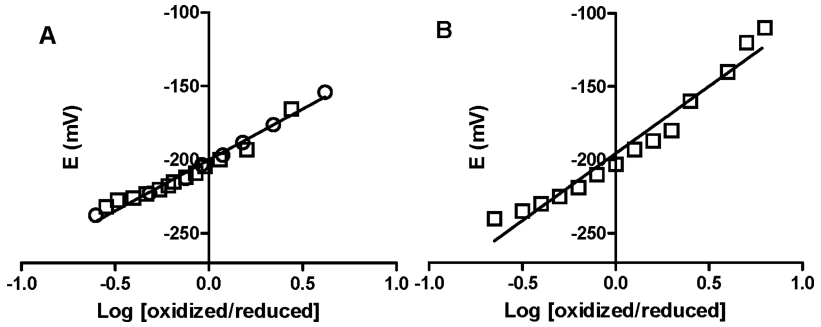

Figure 4. Spectrochemical redox titrations of E113Q MauG (A) and WT MauG (B). Reductive (circles) and oxidative (squares) titrations were performed anaerobically in 50 mM potassium phosphate, pH 7.5, as described in Experimental Procedures. The solid lines are the fits of the data by eq 1.

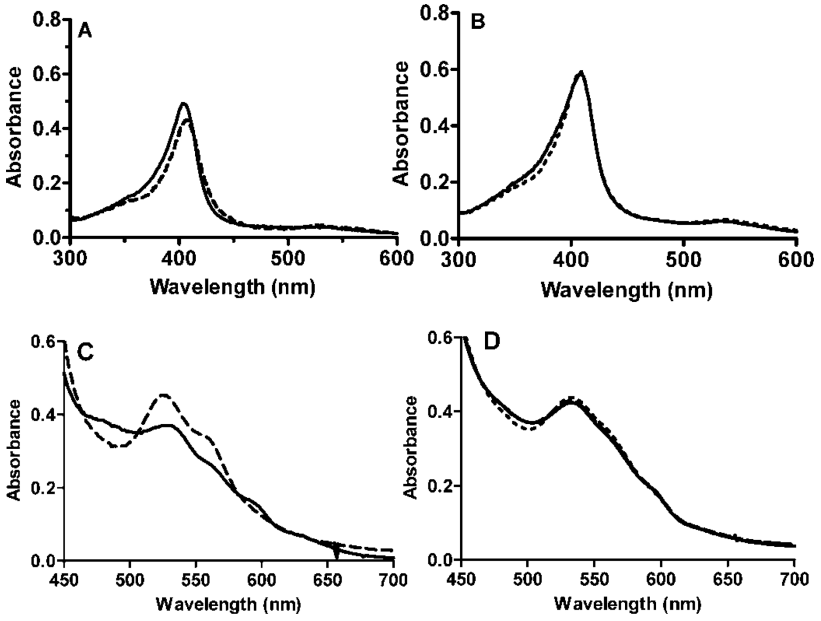

Figure 5. Visible absorption spectra of diferric E113Q MauG before and after addition of H_2O_2. Overlay of the Soret region of the spectra before (solid line) and after (dashed line) addition of a stoichiometric amount of H_2O_2 to 2 μM diferric WT MauG (A) and E113Q MauG (B). Overlay high wavelength visible region of the absorption spectra before (solid line) and after (dashed line) addition of a stoichiometric amount of H_2O_2 to 20 μM diferric WT (C) and E113Q (D) MauG.

cytochrome *c* peroxidases (DCCPs),[32−34] it has not previously been seen in WT MauG or any other mutant MauG proteins.[6,10,11,15,17,23]

Effect of the E113Q Mutation on the E_m values of MauG. Spectrochemical titration of WT MauG exhibits two E_m values of −158 mV and −246 mV, which correspond to the sequential addition or removal of the first and second electrons to or from the diheme system.[23] For reasons that are not clear, the initial reductive titrations of E113Q MauG were routinely not well-behaved; however, after the initial reduction the subsequent oxidative and reductive titrations yielded linear plots that fit well to eq 1 and were reversible and reproducible, yielding an E_m value of −196 ± 6 mV and an *n* value of 1.04 ± 0.10, the latter value consistent with a one-electron oxidation/reduction. This result is consistent with the results of absorbance and resonance Raman spectroscopy, which indicated that only one heme was reduced on addition of excess dithionite. A representative titration is shown in Figure 4A. In contrast to WT MauG, the data for the titration of E113Q was adequately fit by eq 1. For comparison a titration of WT MauG is shown in Figure 4B. Deviation from the linear fit is evident, and the fit yields an *n* value of 0.64 rather than 1.0. For this reason the data for WT MauG, as well as all previously studied MauG variants, were fit by the more complex eq 2, which describes a two-component system and yields two E_m values.

Effects of the E113Q Mutation on the Reaction of MauG with H_2O_2. Reaction of diferric WT MauG with stoichiometric H_2O_2 results in formation of a bis-Fe^{IV} redox state.[8] The formation of the bis-Fe^{IV} species is accompanied by changes in the visible absorbance spectrum, which include a decrease in intensity and a shift of the Soret peak from 406 to 408 nm and appearance of minor peaks at 526 and 559 nm.[14,35] The spectral changes in the Soret peak were not observed after reaction of E113Q MauG with stoichiometric H_2O_2 (Figure 5A,B). Instead, only a small red shift of the left side of the Soret peak was observed. Furthermore, the α/β bands, which presented as two new peaks at 526 and 559 nm in the high-valence form of WT MauG, were absent after addition of H_2O_2 to E113Q MauG (Figure 5C,D). It was previously shown that a Y294H MauG variant did not form the bis-Fe^{IV} state on reaction with H_2O_2 but instead formed a compound I-like

dx.doi.org/10.1021/bi400905s | *Biochemistry* 2013, 52, 6358−6367

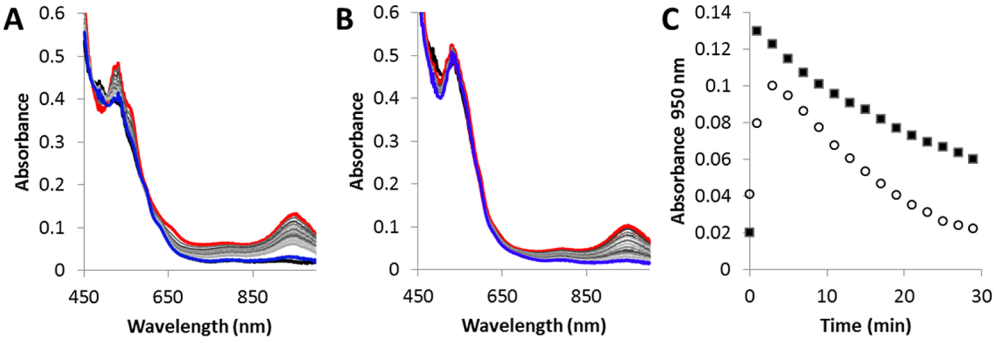

Figure 6. Formation and decay of NIR absorbance features after addition of 10 equiv of H_2O_2 to 20 μM WT MauG (A) and E113Q MauG (B). Spectra were recorded before (bold black traces) and after H_2O_2 addition when the absorbance at 950 nm maximized (bold red traces). Decay was monitored every 2 min (gray scale traces) until no further changes were observed (bold blue traces). (C) Absorbance at 950 nm vs time for WT MauG (solid squares) and E113Q (open circles).

intermediate, which exhibited characteristic absorbance features in the 600−700 nm region.[10] However, no such changes in this region of the spectrum were observed after reaction of H_2O_2 with E113Q MauG (Figure 5D). These data suggest that neither the bis-Fe^{IV} state nor compound I is stabilized by E113Q MauG after reaction with H_2O_2.

To further probe the nature of the high-valence heme species that is formed on addition of H_2O_2 to E113Q MauG, the near-infrared (NIR) region of the absorption spectrum was examined. A NIR absorption feature, which exhibits a maximum at 950 nm, has been described and attributed to a charge-resonance-transition phenomenon involving the two hemes and the intervening Trp93 residue that stabilizes the bis-Fe^{IV} state.[14] In contrast to what was observed in the visible absorbance spectrum, this NIR absorbance feature was observed on addition of 10 equiv of H_2O_2 to E113Q MauG, the conditions that were used in the previous study with WT MauG[14] (Figure 6). In WT MauG, the bis-Fe(IV) species is formed within the dead time of rapid mixing (k > 300 s^{-1}) and spontaneously decays back to the diferric state over several minutes.[35]The formation of the 950 nm absorbance peak in E113Q MauG was much slower (requiring ~4 s) than observed for WT MauG, and the rate of decay was faster (Figure 6C). The intensity of the 950 nm absorbance in the H_2O_2-treated E113Q MauG is also weaker than that of WT MauG.

Effects of the E113Q Mutation on Steady-State Reactions of MauG with Substrates. As the spectroscopic data indicated that reaction of H_2O_2 with E113Q MauG gave rise to some type of high-valence heme species, the reactivity of E113Q MauG was examined using a steady-state assay for TTQ biosynthesis utilizing preMADH and H_2O_2 as the substrates. Whereas WT MauG exhibited a k_{cat} value of 0.2 s^{-1} and K_m value of 1.7 μM for preMADH,[17] no detectable TTQ biosynthesis was observed in this assay with E113Q MauG using up to 20 μM preMADH as the substrate.

Another steady-state assay of MauG uses quinol MADH as a substrate. In this assay MauG is only catalyzing the final two-electron oxidation of TTQ biosynthesis, which is conversion of the quinol to the quinone. With WT MauG, this reaction is significantly faster than the reaction with preMADH and exhibits a k_{cat} of 4.2 s^{-1} and K_m value of 11.1 μM for quinol MADH.[36] Steady-state activity was observed when E113Q MauG was used in this assay, but it was much slower than the reaction of WT MauG and exhibited a k_{cat} value of 0.06 ± 0.01 s^{-1} and K_m value of 17 ± 4 μM (Figure 7).

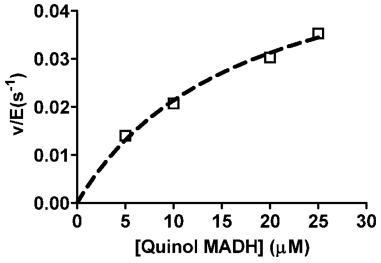

Figure 7. (A) Steady-state E113Q MauG-dependent TTQ biosynthesis utilizing quinol MADH as a substrate. The line is the fit of the data by eq 3.

Structure of the E113Q MauG-preMADH Complex. The crystallographic data collection and refinement statistics are given in Table 1. The overall structure of the E113Q MauG-preMADH protein complex (1.9 Å resolution) is essentially identical to the WT MauG-preMADH structure (rmsd = 0.49 Å over the entire complex). Clear electron density was obtained for the high-spin heme, as well as distal residues and water molecules. Comparison of the high-spin heme environment of E113Q MauG to that of WT MauG shows only a very modest repositioning of Gln113 relative to the WT Glu113 residue (Figure 8). The network of water molecules leading from bulk solvent to the high-spin heme Fe is also unperturbed, and there is no observed change at the low-spin heme. These results are consistent with the very similar spectroscopic properties of diferric WT MauG and E113Q MauG (Figures 2 and 3).

Reactivity of the MauG E113Q-preMADH Complex *in Crystallo*. It was previously shown that the addition of H_2O_2 to crystals of the WT MauG-preMADH complex resulted in completion of TTQ biosynthesis *in crystallo*.[9] In the case of E113Q MauG-preMADH crystals, addition of H_2O_2 appears to result in partial TTQ biosynthesis (Figure 9, Table 1). There has been partial cross-link formation between βTrp57 and βTrp108, but the second oxygen has not been inserted into βTrp57. This result demonstrates that E113Q shows some catalytic activity toward preMADH *in crystallo*.

The H_2O_2-soaked crystal (1.8 Å resolution) contained significant residual difference density at the high-spin heme directly above the heme iron (Supplementary Figure S1). It was not accounted for by the nearest water (W0) observed in the resting state structure, suggesting the presence of a new ligand to the heme Fe. Modeling the site with split occupancy for W0 and a second water molecule modeled into the difference density, followed by refinement, results in a good fit to the

dx.doi.org/10.1021/bi400905s | *Biochemistry* 2013, 52, 6358−6367

Table 1. X-ray Crystallography Data Collection and Refinement Statistics[a]

	E113Q MauG-preMADH resting	E113Q MauG-preMADH + H_2O_2	E113Q MauG-preMADH aged 120 days
Data Collection			
space group	*P*1	*P*1	*P*1
unit cell lengths (Å)	55.95 × 84.90 × 108.50	55.99 × 84.99 × 108.35	55.43 × 83.46 × 107.96
unit cell angles (deg)	110.97, 91.60, 104.62	111.07, 91.82, 104.54	110.15, 91.58, 105.29
wavelength (Å)	1.03313	1.03313	1.03320
resolution (Å)	50.00−1.88 (1.91−1.88)	50.00−1.79 (1.82−1.79)	50.00−2.05 (2.09−2.05)
measured reflections	582,116	706,383	237,068
unique reflections	133,422	168,410	110,039
completeness (%)	97.5 (96.4)	96.4 (83.8)	97.8 (96.3)
R_{merge} (%)[b]	6.6 (48.2)	6.8 (50.8)	6.1 (35.8)
$I/\sigma I$	19.8 (3.4)	20.0 (2.2)	13.4 (2.3)
multiplicity	4.4 (4.4)	4.4 (3.9)	2.2 (2.2)
Refinement			
resolution (Å)	24.35−1.92 (1.97−1.92)	44.49−1.79 (1.84−1.79)	29.62−2.05 (2.10−2.05)
no. reflections; working/test	122,656/6,450	150,844/7,881	101,166/5,334
R_{work} (%)[c]	16.0	15.4	15.8
R_{free} (%)[d]	20.7	19.8	21.0
protein atoms	13,495	13,595	13,329
ligand atoms	213	231	199
solvent sites	1,541	1,488	1,065
Ramachandran statistics[e]			
allowed (%)	98.97	99.13	99.05
outliers (%)	1.03	0.87	0.95
root mean square deviation			
bond lengths (Å)	0.020	0.019	0.018
bond angles (deg)	2.16	2.15	1.96
average *B*-factor (Å^2)	35.97	39.53	37.58
ESU (Å);[f] R_{work}/R_{free}	0.157/0.144	0.117/0.116	0.194/0.168
PDB code	4L1Q	4L3H	4L3G

[a]Values in parentheses are for the highest resolution shell. [b]$R_{merge} = \Sigma_i|I_{hkl,i} - \langle I_{hkl}\rangle|/\Sigma_{hkl}\Sigma_i I_{hkl,i}$, where I is the observed intensity and $\langle I_{hkl}\rangle$ is the average intensity of multiple measurements. [c]$R_{work} = \Sigma||F_o| - |F_c||/\Sigma|F_o|$, where $|F_o|$ is the observed structure factor amplitude, and $|F_c|$ is the calculated structure factor amplitude. [d]R_{free} is the R factor based on 5% of the data excluded from refinement. [e]Based on values attained from refinement validation options in COOT. [f]Estimated standard uncertainties generated for R_{work} and R_{free} in Refmac5.5 in the CCP4i suite.

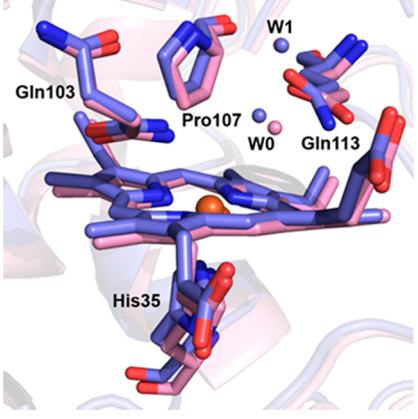

Figure 8. Overlay of the high-spin heme environments of resting WT MauG (pink) and E113Q MauG (blue)-preMADH crystals. Hemes and residues of interest are drawn in sticks colored by atom, with the remaining protein shown in cartoon. The iron is displayed as an orange sphere. Figure produced using PyMOL (http://www.pymol.org/).

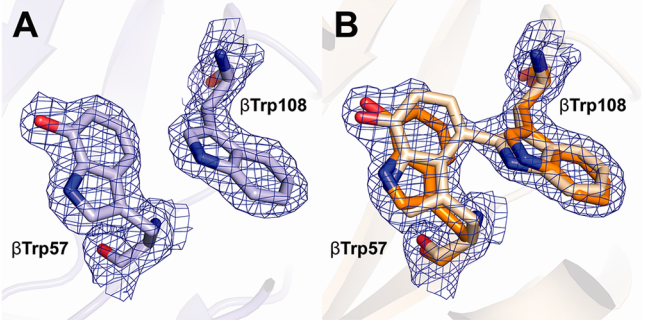

Figure 9. PreTTQ site of β-MADH from (A) resting E113Q MauG-preMADH and (B) H_2O_2-treated E113Q MauG-preMADH. The final model for the H_2O_2-treated E113Q MauG-preMADH contains preTTQ (orange) and cross-linked preTTQ (yellow) each at 50% occupancy. $2F_o - F_c$ electron density is contoured to 1.0 σ. Residues of interest are drawn in sticks colored by atom, with the remaining protein shown in cartoon. Figure produced using PyMOL (http://www.pymol.org/).

resulting $2F_o - F_c$ electron density and similar B-factors for these waters and the heme Fe. With no restraints imposed, the Fe−O distance refines to 1.8 Å, which is long for an Fe(IV)═O bond, being more consistent with compound II[37] and less consistent with WT MauG X-ray absorption data that models a ferryl bond distance of 1.69 Å.[12] Single crystal spectroscopy of a resting state E113Q MauG-preMADH crystal before and after X-ray data collection demonstrated that heme photoreduction is occurring (Supplementary Figure S2). It should be noted that other possible species, such as inclusion of a diatomic ligand, could also be successfully modeled and refined. As such, distal

dx.doi.org/10.1021/bi400905s | *Biochemistry* 2013, 52, 6358−6367

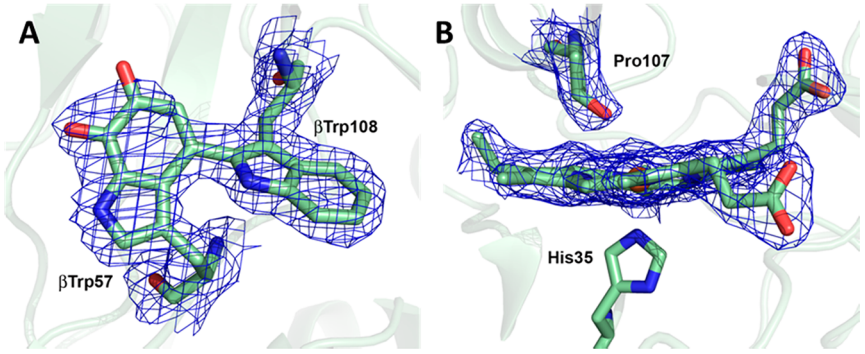

Figure 10. Structure of an E113Q MauG-preMADH crystal aged for 120 days showing modification at the (A) preTTQ site and (B) Pro107 of the high-spin heme site. $2F_o - F_c$ electron density contoured to 1.0 σ. Residues of interest are drawn in sticks colored by atom, with the remaining protein shown in cartoon. Figure produced using PyMOL (http://www.pymol.org/).

ligation is likely a mix of species, including those generated through photoreduction.

It was previously shown that crystals of the WT MauG-preMADH complex catalyzed very slow (~120 days) MauG-dependent TTQ formation as a consequence of the slow release of H_2O_2 from the auto-oxidation of the poly(ethylene glycol) used as the precipitant during crystallization.[7,38] Thus, it was of interest to determine the structure from aged (4 months) crystals of the E113Q MauG-preMADH complex (Table 1). Refinement of this structure to 2.05 Å resolution revealed significant changes at the preTTQ site (Figure 10A). Modeling mature TTQ into both β-MADH chains in this structure resulted in a reasonably good fit of the density, although density for the second oxygen atom of TTQ is somewhat weak. The B-factor for this atom is also relatively high, suggesting that TTQ formation may not be 100%. Nevertheless, this result indicates that E113Q is able to slowly catalyze TTQ formation in the crystals under these conditions. In the high-spin heme distal pocket, new electron density was observed associated with Pro107 (Figure 10B). Modeling Pro107 as a hydroxyproline at 100% occupancy in both MauG chains was necessary in order to obtain satisfactory fits of the density at this position. The hydroxyl oxygen refines to 2.9 Å from the heme iron in both chains.

Reaction of the High Valence Form of E113Q MauG with preMADH in Solution under Single-Turnover Conditions. Given the observations of slow and partial TTQ formation *in crystallo*, the oxidation of preMADH by E113Q MauG was studied under single-turnover conditions, which more closely approximate the conditions *in crystallo* than in solution under steady-state conditions. A 10-fold excess of H_2O_2 was added to E113Q MauG and incubated for 3 min to maximize the formation of the high-valence state, followed by addition of a stoichiometric amount of preMADH (in terms of β-subunit). The reaction mixture was then analyzed by mass spectrometry (Figure 11). The reaction resulted in a 12 Da increase in mass for the β-MADH subunit consistent with formation of the TTQ cofactor.[39] Thus, although the high-valence state of E113Q MauG appears to be very inefficient for the steady-state biosynthesis of TTQ from preMADH in solution, it is not completely inactive.

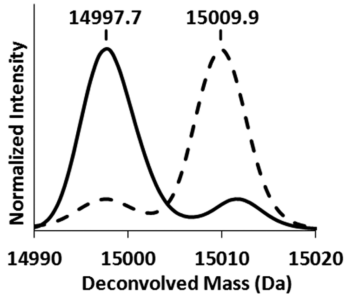

Figure 11. Deconvolved mass spectra of β-preMADH before (solid line) and after (broken line) incubation with stoichiometric E113Q MauG in the presence of a 10-fold excess of H_2O_2.

DISCUSSION

A distinguishing feature of MauG is that it possesses two hemes that are physically separated yet function as a single two-electron diheme redox center. During the interconversion between the diferric and diferrous states the two hemes reduce and oxidize simultaneously.[23] The two E_m values associated with this redox couple do not describe the one-electron redox couples for each individual heme but rather describe the addition or removal of the first and second electron from the diheme system. A mixed-valence state of MauG with one ferric heme while the other one is ferrous has never been observed.[6] Similarly the conversion of the two hemes from the diferric state to the bis-Fe^{IV} state occurs simultaneously.[8] It was recently shown that the formation and relatively long lifetime of the bis-Fe^{IV} state of MauG is achieved through charge-resonance stabilization.[14] This was explained by a hopping mechanism of electron transfer between hemes that is mediated by the intervening Trp93 residue. The very rapid and reversible electron transfer mimics the distribution of charges and spins that would be observed in an extended conjugated system. In this model the bis-Fe^{IV} state is the dominant species, but it is in charge resonance with compound ES and compound I-like species of the high-spin heme.[14] According to this model, the electrostatic environment of the hemes will likely influence the stability of the bis-Fe^{IV} state, as the addition or removal of a charge from a heme site could alter the distribution of the charge-resonance structures such that bis-Fe^{IV} is no longer the dominant species. By analogy, alteration of the electrostatic environment of one of the heme sites might also disrupt the redox cooperativity between the hemes that describes the diferric-diferrous redox couple (discussed below). It should be noted that the 950 nm peak in the NIR spectrum derives from a charge-resonance transition phenomenon that is correlated with an ensemble of resonance structures that includes bis-Fe^{IV}. Thus, the magnitude of this peak does not necessarily correlate with the proportion of bis-Fe^{IV} (or any one resonance

dx.doi.org/10.1021/bi400905s | *Biochemistry* 2013, 52, 6358−6367

structure) within the ensemble. The features of the visible absorbance spectrum of the high-valence state of E113Q MauG indicate that bis-Fe^{IV} is no longer the major species. However, despite the lower proportion of bis-Fe^{IV} species, the presence of the 950 band indicates that a resonance ensemble is still generated upon addition of H_2O_2, but with a different distribution of structures than is present in the high-valence state of WT MauG.

MauG is distinct from the DCCPs and diheme and multiheme cytochromes in that it does not stabilize a mixed-valence Fe^{II}/Fe^{III} state.[32,34] When Glu113 is mutated to Gln, MauG is unable to form the diferrous state and may only be reduced by one electron to a mixed-valence state. This is not due to a change in the structure of the protein (Figure 8). The only significant difference that results from this conservative mutation is the loss of a negative charge in the proximity of the high-spin heme. Yet this change prevents the low-spin heme from being reduced by dithionite. Very little is known of the redox properties of His-Tyr ligated hemes because of their scarcity. The extracellular heme-binding protein HasA, which coordinates a *b*-type heme *via* His and Tyr residues,[40] is reported to have an E_m value of −550 mV for the bound heme.[41] The results obtained for E113Q MauG suggest that this mutation causes disruption of the cooperative redox behavior of MauG, such that the hemes no longer function as a diheme unit but instead now function as independent redox centers. If as a consequence of the loss of redox cooperativity the Tyr-His ligated heme of E113Q MauG has an E_m value similar to that of the HasA-bound heme, then this could explain why it is not reduced by dithionite that has a redox potential in the same range. The expectation that the low-spin heme of MauG would have a very negative E_m value, if functioning independently of the high-spin heme, is supported by X-ray absorption and density functional theory studies that showed that the heme ligand in WT MauG is the deprotonated tyrosinate in all redox states.[12] The sum of these data suggests that the electronic communication between hemes in the diheme redox center of WT MauG not only requires the intervening Trp93 residue but is also dependent on the electrostatic environment of the distal heme pocket of the high-spin heme.

MauG exhibits approximately 30% sequence homology to DCCPs,[1] and residues in the distal pocket of the high-spin heme, including Glu113, are structurally conserved.[9] Glu113 of *P. denitrificans* MauG is equivalent to Glu103 in *Nitrosomonas europaea* DCCP,[21] Glu117 in *Rhodobacter capsulatus* DCCP,[19] and Glu114 in *Pseudomonas nautica* DCCP.[20] This feature has also been described in the mono heme-dependent enzyme *Caldariomyces fiimago* chloroperoxidase, where Glu183 has been suggested to play a role in catalysis by acting as a general base that promotes the heterolytic cleavage of the O−O bond from the hydroperoxy intermediate.[22]

In MauG, Glu113 may act as a proton acceptor during the initial reaction of H_2O_2 with the diferric high-spin heme to generate the ferric hydroperoxy species. The protonated Glu113 then could act as a proton donor to that species leading to heterolytic cleavage of the O−O bond to release water and generate the bis-Fe^{IV}. The crystal structures of CO- and NO-bound adducts of MauG indicated that Glu113 was in a position to serve as a proton donor to the terminal bound O, either directly or via a hydrogen-bonded network of waters.[18] Unlike Glu113, Gln113 would not be able to directly act as an acid−base and could also perturb the pK_a of ordered waters, affecting their ability to act in this capacity, particularly as a proton source. This could explain the observed aberrant reactivity toward H_2O_2 and much slower formation of the high-valence state in E113Q MauG (Figure 6C). As there is no amino acid in the distal pocket that could directly act as an acid−base in the absence of Glu113, it is likely that a water acts in this capacity, although not as efficiently.

The effects of the E113Q MauG on TTQ biosynthesis activity in solution and *in crystallo* may be explained in the context of the charge-resonance-transition model for bis-Fe^{IV} stabilization in MauG, which was described earlier.[14] A consequence of this model is that replacement of amino acid residues in close proximity to either heme may influence the distribution of the resonance structures. It is proposed that the loss of the negative charge in the high-spin heme distal pocket of E113Q MauG alters the distribution of resonance structures such that the bis-Fe^{IV} state is no longer the dominant species. As such it exists for only a small percentage of the time, and this unfavorable resonance equilibrium for bis-Fe^{IV} stabilization limits the availability of the bis-Fe^{IV} species, thus reducing the rate of its reaction. The E113Q mutation causes an approximately 1000-fold decrease in the efficiency of the steady-state oxidation of quinol MADH. For WT MauG, the steady-state biosynthetic reaction with preMADH is much slower than the reaction with quinol MADH, due to a much lower driving force for the former reaction. If the E113Q mutation causes a similar reduction in the rate of the reaction with preMADH, which is 0.2 s^{-1} for WT MauG, then the decreased rate for the reaction of E113Q MauG would be less than that of the spontaneous decay of bis-Fe^{IV} to the diferric state. Furthermore, the NIR spectroscopic data indicates that the rate of spontaneous decay for the high-valence state of E113Q MauG is faster than that for WT MauG (Figure 6C). This explains why no reaction is detectable in the steady-state reaction with preMADH in solution, because the high-valence species decays faster than it reacts with preMADH. However, increasing the relative concentration of E113Q MauG overcomes this deficiency, resulting in turnover as determined by mass spectrometry (Figure 11). *In crystallo* the bis-Fe^{IV} state may also be stabilized because of reduced dynamics imposed by the crystal lattice allowing a slow reaction with preMADH to be observed.

The susceptibility of Pro107 to oxidation in aged E113Q MauG crystals is also interesting because Pro107 occupies a very similar position to the substrate in the structure of substrate-bound cytochrome P450cam.[9,42] The same rationale for why TTQ biosynthesis is observed *in crystallo* but not in solution can be applied to the observation of hydroxylation of Pro107 *in crystallo*. During the spontaneous decay of bis-Fe^{IV}, this species must acquire electrons from some donor, which is most likely buffer. However, it is not unreasonable to believe that if this process is repeated enough times, then it may sometimes instead extract an electron from Pro107, which will result in oxidative modification. The initial oxidation of Pro107 to generate a cation radical would be reversible, but further reaction of the resultant radical with water would irreversibly yield hydroxylated Pro107. In solution, H_2O_2 causes general oxidative damage and inactivation of WT MauG after a few cycles of bis-Fe^{IV} formation and decay.[43] In the aged crystal, where H_2O_2 is slowly released over a 4 month period, 100% hydroxylation of Pro107 is observed with minimal evidence of other oxidative damage and no chemical damage to the hemes. In this context the crystals of E113Q MauG appear to be robust

dx.doi.org/10.1021/bi400905s | *Biochemistry* 2013, 52, 6358−6367

in their tolerance to long-term H_2O_2 exposure, either through crystal packing effects or the crystal mother liquor, or both. Hydroxylation of Pro107 was not observed in similarly aged crystals of the WT MauG-preMADH complex, in which complete formation of TTQ was observed.[7] Thus, the oxidative modification of Pro107 *in crystallo* does appear to be a consequence of the altered reactivity of MauG toward H_2O_2 and preMADH, as described in the solution studies.

■ ASSOCIATED CONTENT

Supporting Information

Figures S1 and S2. This material is available free of charge via the Internet at http://pubs.acs.org.

Accession Codes

Coordinates and structure factors have been deposited in the Protein Data Bank as 4L1Q (E113Q MauG-preMADH), 4L3H (E113Q MauG-preMADH + H_2O_2), and 4L3G (E113Q MauG-preMADH, aged 120 days).

■ AUTHOR INFORMATION

Corresponding Author

*Tel: 407-266-7111. Fax: 407-266-7002. E-mail: victor.davidson@ucf.edu.

Funding

This research was supported by the National Institute of General Medical Sciences of the National Institutes of Health under award numbers R37GM41574 (V.L.D.), R01GM66569 (C.M.W.), and F32GM97779 (E.T.Y.), a Minnesota Partnership for Biotechnology and Medical Genomics Grant SPAP-05-0013-P-FY06 (C.M.W.) and partial support from the HHMI seed grant at Tougaloo College (M.F.).

Notes

The authors declare no competing financial interest.

■ ACKNOWLEDGMENTS

Computer resources were provided by the Basic Sciences Computing Laboratory of the University of Minnesota Supercomputing Institute, and we thank Nancy Rowe for her support. X-ray data were collected at the Kahlert Structural Biology Laboratory (KSBL) at The University of Minnesota and GM/CA-CAT at the Advanced Photon Source (APS), Argonne National Laboratory, Argonne, IL. GM/CA CAT has been funded in whole or in part with Federal funds from the National Cancer Institute (Y1-CO-1020) and the National Institute of General Medical Science (Y1-GM-1104). Use of the APS was supported by the U.S. Department of Energy, Basic Energy Sciences, Office of Science, under contract No. DE-AC02-06CH11357. We thank Ed Hoeffner for KSBL support, and the staff at Sector 23, APS for their support. Resonance Raman spectra were collected at the Analytical Core Laboratory (RCMI core facility) at Jackson State University.

■ ABBREVIATIONS

TTQ, tryptophan tryptophylquinone; preMADH, the biosynthetic precursor protein of MADH with incompletely synthesized TTQ; bis-Fe(IV) MauG, redox state of MauG with one heme as Fe(IV)=O and the other as Fe(IV); WT, wild-type; DCCP, diheme cytochrome *c* peroxidase; NIR, near-infrared

■ REFERENCES

(1) Wang, Y., Graichen, M. E., Liu, A., Pearson, A. R., Wilmot, C. M., and Davidson, V. L. (2003) MauG, a novel diheme protein required for tryptophan tryptophylquinone biogenesis. *Biochemistry 42*, 7318−7325.

(2) Davidson, V. L. (2007) Protein-derived cofactors. Expanding the scope of post-translational modifications. *Biochemistry 46*, 5283−5292.

(3) Davidson, V. L. (2011) Generation of protein-derived redox cofactors by posttranslational modification. *Mol. Biosyst. 7*, 29−37.

(4) Davidson, V. L. (2001) Pyrroloquinoline quinone (PQQ) from methanol dehydrogenase and tryptophan tryptophylquinone (TTQ) from methylamine dehydrogenase. *Adv. Protein Chem. 58*, 95−140.

(5) Pearson, A. R., De La Mora-Rey, T., Graichen, M. E., Wang, Y., Jones, L. H., Marimanikkupam, S., Agger, S. A., Grimsrud, P. A., Davidson, V. L., and Wilmot, C. M. (2004) Further insights into quinone cofactor biogenesis: probing the role of *mauG* in methylamine dehydrogenase tryptophan tryptophylquinone formation. *Biochemistry 43*, 5494−5502.

(6) Davidson, V. L., and Wilmot, C. M. (2013) Posttranslational biosynthesis of the protein-derived cofactor tryptophan tryptophylquinone. *Annu. Rev. Biochem. 82*, 531−550.

(7) Yukl, E. T., Liu, F., Krzystek, J., Shin, S., Jensen, L. M., Davidson, V. L., Wilmot, C. M., and Liu, A. (2013) Diradical intermediate within the context of tryptophan tryptophylquinone biosynthesis. *Proc. Natl. Acad. Sci. U.S.A. 110*, 4569−4573.

(8) Li, X., Fu, R., Lee, S., Krebs, C., Davidson, V. L., and Liu, A. (2008) A catalytic di-heme bis-Fe(IV) intermediate, alternative to an Fe(IV)=O porphyrin radical. *Proc. Natl. Acad. Sci. U.S.A. 105*, 8597−8600.

(9) Jensen, L. M., Sanishvili, R., Davidson, V. L., and Wilmot, C. M. (2010) In crystallo posttranslational modification within a MauG/pre-methylamine dehydrogenase complex. *Science 327*, 1392−1394.

(10) Abu Tarboush, N., Jensen, L. M., Feng, M., Tachikawa, H., Wilmot, C. M., and Davidson, V. L. (2010) Functional importance of tyrosine 294 and the catalytic selectivity for the bis-Fe(IV) state of MauG revealed by replacement of this axial heme ligand with histidine. *Biochemistry 49*, 9783−9791.

(11) Abu Tarboush, N., Shin, S., Geng, J., Liu, A., and Davidson, V. L. (2012) Effects of the loss of the axial tyrosine ligand of the low-spin heme of MauG on its physical properties and reactivity. *FEBS Lett. 586*, 4339−4343.

(12) Jensen, L. M., Meharenna, Y. T., Davidson, V. L., Poulos, T. L., Hedman, B., Wilmot, C. M., and Sarangi, R. (2012) Geometric and electronic structures of the His-Fe(IV)=O and His-Fe(IV)-Tyr hemes of MauG. *J. Biol. Inorg. Chem. 17*, 1241−1255.

(13) Ling, Y., Davidson, V. L., and Zhang, Y. (2010) Unprecedented Fe(IV) species in a diheme protein MauG: A quantum chemical investigation on the unusual Mössbauer spectroscopic properties. *J. Phys. Chem. Lett. 1*, 2936−2939.

(14) Geng, J., Dornevil, K., Davidson, V. L., and Liu, A. (2013) Tryptophan-mediated charge-resonance stabilization in the bis-Fe(IV) redox state of MauG. *Proc. Natl. Acad. Sci. U.S.A. 110*, 9639−9644.

(15) Abu Tarboush, N., Jensen, L. M. R., Yukl, E. T., Geng, J., Liu, A., Wilmot, C. M., and Davidson, V. L. (2011) Mutagenesis of tryptophan199 suggets that hopping is required for MauG-dependent tryptophan tryptophylquinone biosynthesis. *Proc. Natl. Acad. Sci. U.S.A. 108*, 16956−16961.

(16) Choi, M., Shin, S., and Davidson, V. L. (2012) Characterization of electron tunneling and hole hopping reactions between different forms of MauG and methylamine dehydrogenase within a natural protein complex. *Biochemistry 51*, 6942−6949.

(17) Feng, M., Jensen, L. M., Yukl, E. T., Wei, X., Liu, A., Wilmot, C. M., and Davidson, V. L. (2012) Proline 107 is a major determinant in maintaining the structure of the distal pocket and reactivity of the high-spin heme of MauG. *Biochemistry 51*, 1598−1606.

(18) Yukl, E. T., Goblirsch, B. R., Davidson, V. L., and Wilmot, C. M. (2011) Crystal structures of CO and NO adducts of MauG in complex with pre-methylamine dehydrogenase: Implications for the mechanism of dioxygen activation. *Biochemistry 50*, 2931−2938.

(19) De Smet, L., Savvides, S. N., Van Horen, E., Pettigrew, G., and Van Beeumen, J. J. (2006) Structural and mutagenesis studies on the cytochrome *c* peroxidase from *Rhodobacter capsulatus* provide new insights into structure-function relationships of bacterial di-heme peroxidases. *J. Biol. Chem. 281*, 4371−4379.
(20) Dias, J. M., Alves, T., Bonifacio, C., Pereira, A. S., Trincao, J., Bourgeois, D., Moura, I., and Romao, M. J. (2004) Structural basis for the mechanism of Ca(2+) activation of the di-heme cytochrome *c* peroxidase from Pseudomonas nautica 617. *Structure 12*, 961−973.
(21) Shimizu, H., Schuller, D. J., Lanzilotta, W. N., Sundaramoorthy, M., Arciero, D. M., Hooper, A. B., and Poulos, T. L. (2001) Crystal structure of *Nitrosomonas europaea* cytochrome *c* peroxidase and the structural basis for ligand switching in bacterial di-heme peroxidases. *Biochemistry 40*, 13483−13490.
(22) Sundaramoorthy, M., Terner, J., and Poulos, T. L. (1995) The crystal structure of chloroperoxidase: a heme peroxidase−cytochrome P450 functional hybrid. *Structure 3*, 1367−1377.
(23) Li, X., Feng, M., Wang, Y., Tachikawa, H., and Davidson, V. L. (2006) Evidence for redox cooperativity between *c*-type hemes of MauG which is likely coupled to oxygen activation during tryptophan tryptophylquinone biosynthesis. *Biochemistry 45*, 821−828.
(24) Li, X., Jones, L. H., Pearson, A. R., Wilmot, C. M., and Davidson, V. L. (2006) Mechanistic possibilities in MauG-dependent tryptophan tryptophylquinone biosynthesis. *Biochemistry 45*, 13276−13283.
(25) Otwinowski, Z., and Minor, W. (1997) Processing of X-ray diffraction data collected in oscillation mode. *Methods Enzymol. 276*, 307−326.
(26) Murshudov, G. N., Vagin, A. A., and Dodson, E. J. (1997) Refinement of macromolecular structures by the maximum-likelihood method. *Acta Crystallogr., Sect. D: Biol. Crystallogr. 53*, 240−255.
(27) CCP4 (1994) Collaborative Computational Project Number 4, *Acta Crystallogr. Sect. D Biol. Crystallogr. 50*, 760−763.
(28) Emsley, P., and Cowtan, K. (2004) Coot: model-building tools for molecular graphics. *Acta Crystallogr., Sect. D: Biol. Crystallogr. 60*, 2126−2132.
(29) Hu, S., Morris, I. K., Singh, J. P., Smith, K. M., and Spiro, T. G. (1993) Complete assignment of cytochrome *c* resonance raman spectra via enzymatic reconstitution with isotopically labeled heme. *J. Am. Chem. Soc. 115*, 12446−12458.
(30) Tu, A. T. (1982) in *Raman Spectroscopy in Biology; Principles and Applications*; pp 331−337, John Wiley and Sons Inc., New York.
(31) Desbois, A. (1994) Resonance Raman spectroscopy of *c*-type cytochromes. *Biochimie 76*, 693−707.
(32) Fulop, V., Watmouth, N. J., and Ferguson, S. J. (2001) Structure and enyzmology of two bacterial diheme enzymes: cytochrome cd_1 nitrite reductase and cytochrome *c* peroxidase. *Adv. Inorg. Chem. 51*, 163−204.
(33) Pettigrew, G. W., Echalier, A., and Pauleta, S. R. (2006) Structure and mechanism in the bacterial dihaem cytochrome *c* peroxidases. *J. Inorg. Biochem. 100*, 551−567.
(34) Wilmot, C. M., and Davidson, V. L. (2009) Uncovering novel biochemistry in the mechanism of tryptophan tryptophylquinone cofactor biosynthesis. *Curr. Opin. Chem. Biol. 13*, 469−474.
(35) Lee, S., Shin, S., Li, X., and Davidson, V. (2009) Kinetic mechanism for the initial steps in MauG-dependent tryptophan tryptophylquinone biosynthesis. *Biochemistry 48*, 2442−2447.
(36) Shin, S., Abu Tarboush, N., and Davidson, V. L. (2010) Long range electron transfer reactions between hemes of MauG and different forms of tryptophan tryptophylquinone of methylamine dehydrogenase. *Biochemistry 49*, 5810−5816.
(37) Gumiero, A., Metcalfe, C. L., Pearson, A. R., Raven, E. L., and Moody, P. C. (2011) Nature of the ferryl heme in compounds I and II. *J. Biol. Chem. 286*, 1260−1268.
(38) Hamburger, R., Azaz, E., and Donbrow, M. (1975) Autoxidation of polyoxyethylenic nonionic surfactants and of polyethylene glycols. *Pharm. Acta Helv. 50*, 10−17.
(39) Wang, Y., Li, X., Jones, L. H., Pearson, A. R., Wilmot, C. M., and Davidson, V. L. (2005) MauG-dependent in vitro biosynthesis of tryptophan tryptophylquinone in methylamine dehydrogenase. *J. Am. Chem. Soc. 127*, 8258−8259.
(40) Arnoux, P., Haser, R., Izadi, N., Lecroisey, A., Delepierre, M., Wandersman, C., and Czjzek, M. (1999) The crystal structure of HasA, a hemophore secreted by *Serratia marcescens*. *Nat. Struct. Biol. 6*, 516−520.
(41) Izadi, N., Henry, Y., Haladjian, J., Goldberg, M. E., Wandersman, C., Delepierre, M., and Lecroisey, A. (1997) Purification and characterization of an extracellular heme-binding protein, HasA, involved in heme iron acquisition. *Biochemistry 36*, 7050−7057.
(42) Raag, R., and Poulos, T. L. (1991) Crystal structures of cytochrome P-450CAM complexed with camphane, thiocamphor, and adamantane: factors controlling P-450 substrate hydroxylation. *Biochemistry 30*, 2674−2684.
(43) Shin, S., Lee, S., and Davidson, V. L. (2009) Suicide inactivation of MauG during reaction with O_2 or H_2O_2 in the absence of its natural protein substrate. *Biochemistry 48*, 10106−10112.